7-5 The AMATERASU Scattering Module

Jana Mendrok, Philippe Baron, and KASAI Yasuko

We introduce the cloud case version of the Advanced Model for Atmospheric Terahertz Radiation Analysis and Simulation (AMATERASU) that has been developed in the framework of the NICT Terahertz project. The current status of the cloudy atmosphere modules, that have a strong heritage from the [Approximate] Spherical Atmospheric Radiative Transfer (SARTre) model, is described with a focus on new developments for the Terahertz spectral region. Deviations of model approaches from clear-sky AMATERASU are discussed and future plans are pointed out.

Keywords
Atmospheric radiative transfer, Scattering, Terahertz, Far-Infrared, Ice clouds

1 Introduction

The Terahertz (THz) or Far-Infrared (FIR) region (0.1 – 20 THz ≈ 3 – 670 cm^{-1} ≈ 3000 – 15 μm) of the electromagnetic spectrum is a rather unexplored spectral region for atmospheric research. Situated in the transition zone between radio wave and optoelectronic regimes this is mainly due to technological reasons.

However, this previous inability to observe this region does not coincide with the importance of the THz region for atmospheric processes and their observation, for the global energy budget and Earth's climate. In particular, 50 % of the total outgoing longwave radiation (OLR) and even 75 % of the atmospheric part of the OLR are concentrated in this spectral region. Furthermore, it is known that cirrus as well as longwave cloud radiative forcing have major components in the THz region. Although we gained a good idea about the crucial role this spectral region plays in the Earth-atmosphere system, we still lack precise knowledge and a global view of the absolute values[1].

Beside that, the THz region is also of high interest for observation and monitoring of ice clouds, which play a key role not only in the energy budget but also in the hydrological cycle that is closely linked with Earth's climate. Great progress in cloud ice monitoring has recently been gained based on a number of instruments on the so-called A-train, and CloudSat in particular. However, there are still a number of limitations that restrict accuracies in ice content measurements to about 200 %. With its wavelength being in the order of the size of ice particles, the THz region is highly sensitive to cloud ice. While the lower frequencies are mainly sensitive to the size mode where most of the ice is concentrated (≈ 50 – 200 μm), the usage of higher frequencies allows for a "scanning" of the size distribution, i.e., for the derivation of microphysical information, as well as for higher altitude resolution. In conclusion, THz observations are highly promising for improving measurements of several important ice cloud properties.

Along with the growing ability of observations in the THz range, there is a need for updated and improved radiative transfer models in order to be able to simulate and analyze the measurements. Here, we present recent developments in radiative transfer modeling for the Far-Infrared/Terahertz range. The

Advanced Model for Atmospheric TeraHertz Radiation Analysis and Simulation (AMATERASU), developed within the TeraHertz Project at NICT is introduced. While Baron et al.[2] describe the modules for clear-sky THz calculations, in this article we focus on the AMATERASU modules dealing with atmospheres that contain atmospheric particles, e.g., water droplets or ice particles as can be found in clouds. Concerning radiative transfer that means, these modules consider emission/absorption as well as scattering as sources/sinks of radiation.

The fundamental principles of radiative transfer (RT) with scattering are introduced in Section **2** along with their implementation in AMATERASU. Sections **3** and **4** focus on the methods implemented in AMATERASU to obtain optical properties of ensembles of atmospheric particles, which are a crucial parameter in radiative transfer calculations. In particular, that includes the derivation of scattering and absorption properties of ice particles found in high altitude clouds. Conclusions are drawn in section **5**.

2 The AMATERASU scattering module

AMATERASU has been developed with a strong heritage from the models Moliere[3] and SARTre[4]. The Moliere heritage of AMATERASU comprises modules dealing with calculation of molecular absorption coefficients and weighting functions as well as application of instrumental line shape, etc., and modules related to optical properties of atmospheric particles and to scattering have been adapted from SARTre.

While a full integration of modules from both source models is planned, currently they coexist rather independently with a number of external routines allowing for the flow of data between the two kind of modules. For example, the solution of the radiative transfer equation is derived using slightly different approaches for clear-sky and cloudy cases, with the former using modules coming from Moliere and the latter involving SARTre modules. Both, Moliere and SARTre modules of AMATERASU have been adapted for RT calculations in the THz spectral range. However, several AMATERASU modules like those providing weighting functions, dealing with instrumental features, or performing retrievals that work for clear-sky cases are not yet applicable to cloud cases with the current version of AMATERASU.

The following subsections describe the algorithms for cloud case RT as used at the moment within AMATERASU with a focus on changes of the modules taken from SARTre that have been implemented for calculations in the THz region. While the approach to the solution of the radiative transfer equation has not been changed, adaptions to THz region concentrate in the field of deriving the optical properties of atmospheric particles.

2.1 Radiative transfer equation

Like Moliere and the clear-sky version of AMATERASU, SARTre and the cloud version of AMATERASU apply the source function integration technique. Using the integral radiative transfer equation

$$I(\nu) = I_{\mathrm{b}}(\nu)\,\mathrm{e}^{-\tau(\nu)} + \int_0^{\tau(\nu)} J(\tau',\nu)\,\mathrm{e}^{-\tau'(\nu)}\,\mathrm{d}\tau' \quad (1)$$

radiation sources J are "collected" along the observer line of sight (LoS) and transmitted to the instrument following Beer's law. Here $I(\nu)$ is the monochromatic intensity at wavenumber ν and I_{b} denotes background radiation, e.g., emission from the surface or the cold space. τ is the optical depth of the medium measured from the observer along the LoS.

In contrast to the clear-sky AMATERASU modules that assumes homogeneous layers between the grid points along the LoS (compare Eq. (3) in Baron et al.[2]), the cloud version assumes linear evolution of the source terms J_{n} within each path segment. Splitting the LoS into N path segments, Eq. (1) can be rewritten as

$$I = I_b\, e^{-\sum_{n=1}^{N}\Delta\tau_n} + \sum_{n=1}^{N}\left(e^{-\sum_{m=1}^{n-1}\Delta\tau_m}\int_0^{\Delta\tau_n} J_n\, e^{-\Delta\tau'}\,\mathrm{d}\Delta\tau'\right) \quad (2)$$

with $\Delta\tau_n$ being the path optical depth of segment n. Contributions J_n from the individual path segments can be expressed in terms of source terms evaluated at discrete path grid points and coefficients depending on the path segment's optical depth:

$$\int_0^{\Delta\tau_n} J_n\, e^{-\Delta\tau'}\,\mathrm{d}\Delta\tau' = a_{1,n}\, J_n(0) + a_{2,n}\, J_n(\Delta\tau_n) \quad (3)$$

with

$$a_{1,n} = \int_0^{\Delta\tau_n} \frac{\Delta\tau_n - \Delta\tau'}{\Delta\tau_n} e^{-\Delta\tau'}\,\mathrm{d}\Delta\tau' \quad \text{and}$$
$$a_{2,n} = \int_0^{\Delta\tau_n} \frac{\Delta\tau'}{\Delta\tau_n} J_n(\Delta\tau_n) e^{-\Delta\tau'}\,\mathrm{d}\Delta\tau'. \quad (4)$$

that can be solved analytically when linearity of J within the path segment is assumed. When further defining

$$a_{0,n} = e^{-\sum_{m=1}^{n-1}\Delta\tau_m} \quad (5)$$

then Eq. (2) can finally be written as

$$I = I_b\, a_{0,N} + \sum_{n=1}^{N} a_{0,n}\,(a_{1,n}\, J_n(0) + a_{2,n}\, J_n(\Delta\tau_n)). \quad (6)$$

Concerning accuracy of the quadrature, the line of sight has to be split into appropriately small path segments over which linearity can be assumed.

2.2 Path optical depth in a spherical atmosphere

In Eqs. (2)-(6) $\Delta\tau$ describes the extinction, integrated along a path segment, which is caused by molecular absorption on the one hand and scattering as well as absorption by particles on the other. Optical properties of gaseous matter, which are provided by Moliere-heritage modules of AMATERASU (for details see Baron et al.[2]), and those of particles can be handled separately, i.e., for $\Delta\tau$ applies

$$\Delta\tau = \Delta\tau^{\mathrm{mol}} + \Delta\tau^{\mathrm{par}}, \quad (7)$$

where $\Delta\tau^{\mathrm{mol}}$ is the optical depth of the gaseous matter and $\Delta\tau^{\mathrm{par}}$ denotes the particle optical depth. From particle and molecular extinction that are commonly given with respect to altitude z optical depth along a path segment $\Delta\tau_s$ needs to be derived. In a spherical atmosphere, vertical thickness and path length through a path segment, Δz and Δs respectively, relate to each other by the so-called Chapman function[5], which may generally not be evaluated analytically. The commonly used approximation [e.g., [6]] of $\Delta\tau_s = \Delta\tau_z \cdot \Delta s/\Delta z$ is critical concerning accuracy, particulary for large zenith angles that occur close to the tangent point of limb LoS. For AMATERASU cloud modules, a second order polynomial is assumed to describe the dependence of extinction on the position along the path

$$\beta_e(\Delta s) = a \cdot \Delta s^2 + b \cdot \Delta s + c. \quad (8)$$

Coefficients a, b, and c are derived for individual path segments from extinction coefficients at the boundary of each segment and a third point at mean segment altitude. From $\tau = \int \beta_e\,\mathrm{d}s$ and Eq. (8) follows

$$\Delta\tau_s = \frac{a}{3} \cdot \Delta s^3 + \frac{b}{2} \cdot \Delta s^2 + c \cdot \Delta s. \quad (9)$$

2.3 Source terms

The term $J = J_B + J_{MS}$ contains the sources of radiation originating from thermal emission (B) and multiple scattering (MS) with

$$J_B = (1 - \omega_0)\, B(T) \quad (10)$$

$$J_{MS} = \omega_0 \frac{1}{4\pi} \int_0^{4\pi} P(\Theta)\, I(\mathbf{\Omega'})\,\mathrm{d}\Omega', \quad (11)$$

where $B(T)$ denotes the Planck emission term, $P(\Theta)$ is the phase function in dependence of the scattering angle and $I(\Omega')$ describes the incident radiation field in terms of incident

direction. ω_0 describes the scattering albedo of the "mixed" atmospheric medium along the the LoS. It is calculated from molecular and particle optical properties by

$$\omega_0 = \frac{\beta_s^{par}}{\beta_s^{par} + \beta_a^{par} + \beta_a^{mol}}, \quad (12)$$

where β_s and β_a are scattering and absorption coefficients with superscripts 'mol' and 'par' denoting properties of molecular and particulate matter, respectively.

While J_B is calculated with full respect to the sphericity of the Earth-atmosphere system, the multiple scattering source term J_{MS} requires the knowledge of the incident radiation field $I(\Omega')$. Assuming a local planarity of the Earth and atmosphere, as indicated by Fig. 1, $I(\Omega')$ is derived within a plan-parallel atmosphere, using the DISORT radiative transfer package[7]. Except for that, source term J_{MS} is handled in a spherical atmosphere as well. That is, contributions from multiple scattering are calculated for local parameter values assigned to the individual grid points along the LoS through a spherical atmosphere, e.g., local direction Ω. Although only set up for a spherical shell atmosphere momentarily, this approach allows for applying an independent pixel approximation based two-dimensional atmosphere with only slight modifications.

The DISORT module solves the radiative transfer problem for a plane-parallel one-dimensional atmosphere being a single slab of constant refractive index. However, vertical inhomogeneity is considered by dividing the slab into a number of homogeneous layers with vertical optical thickness $\Delta\tau_z$, that can be adequately characterized by constant single scattering albedo ω_0^{DIS} and scattering phase function $P(\Theta)$. $\Delta\tau_z$ is calculated by analytic integration of the explicitly given or assumed exponential change of particle and molecular scattering/absorption coefficients, within a layer. Since molecular absorption coefficients are defined at discrete altitudes, single scattering albedo ω_0 as derived from Eq. (12) is not necessarily constant within a layer. For DISORT a representative average single scattering albedo of the layer is calculated by

$$\omega_0^{DIS} = \frac{\Delta\tau_s^{par}}{\Delta\tau^{mol} + \Delta\tau^{par}} = \frac{\int_{z_{min}}^{z_{max}} N(z)\,\sigma_s^{par}\,dz}{\int_{z_{min}}^{z_{max}} N(z)\,(\sigma_s^{par} + \sigma_a^{par})\,dz + \int_{z_{min}}^{z_{max}} \beta_a^{mol}\,dz}, \quad (13)$$

where $\Delta\tau_s^{par}$ denotes the optical depth due to particle scattering, $\Delta\tau^{mol}$ and $\Delta\tau^{par}$ are the total molecular and particle optical depth of the layer, respectively.

3 Optical properties of clouds

Atmospheric particulate matter includes aerosols as well as hydrometeors in clouds (e.g., water droplets and ice particles) and precipitation (e.g., rain, snow, graupel, hail).

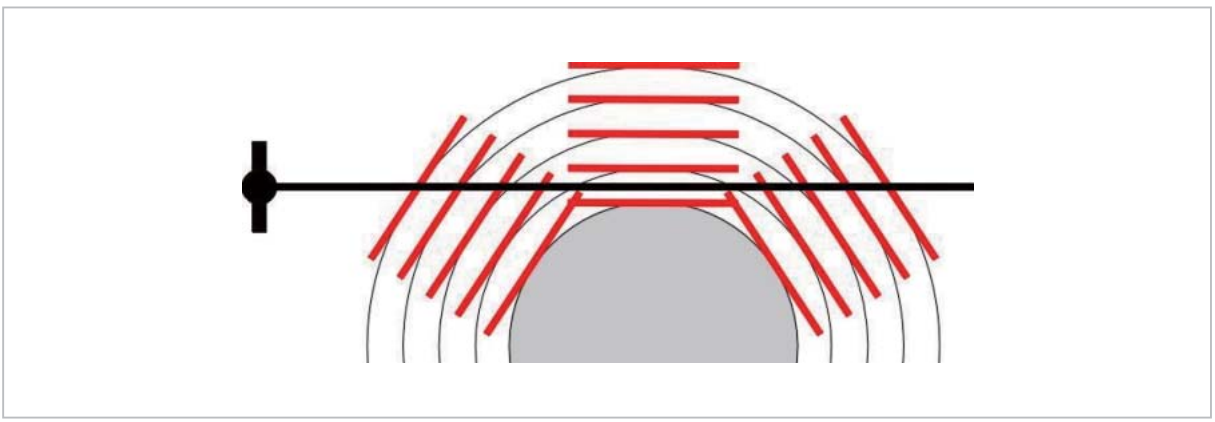

Fig. 1 *Local planarity assumption in a spherical atmosphere. The incident radiation field at grid points along the LoS is derived in a local plane-parallel atmosphere, indicated in red.*

While radiative effects of aerosols can be neglected in the THz range, hydrometeors emit, absorb, and scatter radiation in certain fractions depending on the size and shape of the particles involved. Although precipitating particles are known to modify the transfer of radiation in the atmosphere at the lower frequency end of the THz region, they can not yet be handled with AMATERASU. For liquid and ice cloud particles several methods have been implemented in AMATERASU to derive their optical properties.

Within AMATERASU, atmospheric particles are assumed to occur in homogeneous layers, i.e., optical properties are assumed to be constant over the whole layer in horizontal and vertical direction. To meet this assumption, vertically inhomogeneous parts of the atmosphere have to be divided into sufficiently small layers that can be taken to be homogeneous. In the atmosphere, particles always exist at a range of sizes, and are usually also of different shapes and material, i.e., occur as polydispersions. Most of the models and databases provide optical properties for single particles of a defined size, shape and material only. Those monodispersion properties have to be convolved with functions describing the distribution of particles in the bulk concerning size, shape and material. Scattering by samples of particles are assumed to be independent, i.e., a scattering event at one particle does not interfere with those at other particles. In consequence, scattered intensities may be added without regard to the phases of the individual scattered waves. Thus, bulk optical properties can be obtained by a weighted mean of single particle properties.

For clouds, particles are usually considered to be formed from pure water, i.e., a single material. Ice particles are known to show very different shapes in the atmosphere with a wide variety of shape distributions, which is hard to represent appropriately in models. Therefore, shape distributions are commonly largely simplified, such that only a single shape is assumed, that might be related to temperature or cloud type but is mostly driven or restricted by the abilities to derive single particle properties for various shapes.

Particle size distributions are often expressed as a function $n(a)$ of a few parameters, e.g., the ambient temperature and/or ice water content of an ice cloud. Then, the extinction coefficient of a sample of particles is given by

$$\beta_{\mathrm{e}} = \int_{a_{\min}}^{a_{\max}} n(a)\, \sigma_{\mathrm{e}}(a)\, \mathrm{d}a \qquad (14)$$

with $a_{\min}$ and $a_{\max}$ being the minimum and maximum particle size considered by the distribution, respectively, and $\sigma_{\mathrm{e}}(a)$ denoting the extinction cross section of a particle of dimension a. Scattering as well as absorption coefficients can be calculated analogously. The phase function of a polydispersion is derived from

$$\beta_{\mathrm{s}}\, P(\Theta) = \int_{a_{\min}}^{a_{\max}} n(a)\, \sigma_{\mathrm{s}}(a)\, P(\Theta, a)\, \mathrm{d}a. \qquad (15)$$

Due to the focus of previous studies, currently only size distributions for tropospheric ice clouds taken from Liou[8] and Shettle[9] are implemented in AMATERASU. The distributions from Liou[8] are parameterizations of data from Heymsfield and Platt[10] in terms of ambient temperature. Liou[8] also provides a parameterization of ice water con-

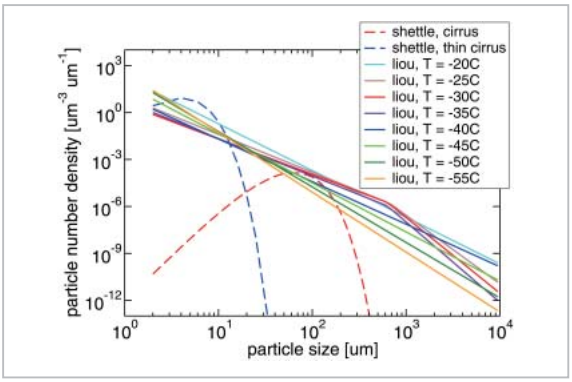

Fig.2 *Particle size distributions for ice clouds as currently implemented in AMATERASU. Originating from Shettle[9] (dashed) and Liou[8] (solid) with the latter plotted for several parameterization temperatures over the defined range. For better comparability, all distributions have been scaled to a constant ice water content.*

tent *IWC* of the cloud in terms of temperature. In Shettle[9] fixed distributions are given for "cirrus" and "thin cirrus". Figure 2 illustrates these distributions.

For future studies, we will implement size distributions for different kinds of liquid water clouds as well. Beside size distributions from Shettle[9] which are the ones implemented in the well-established RT model MODTRAN[11], we will extract size distributions from OPAC[12]. OPAC provides single scattering properties for monodispersions as well as polydispersion of self- and predefined mixtures of ice and water clouds as well as aerosols, but is restricted to wavelengths up to only 10 μm.

For the derivation of monodispersion optical properties Lorentz-Mie theory can be applied assuming sphericity of the particles. This is a good approximation for non-precipitating water droplets, but is also used frequently for ice particles when observed at lower frequencies. In AMATERASU a Lorentz-Mie-code by Wiscombe[13] has recently been implemented, that provides optical properties of monodispersions including absorption and scattering efficiencies as well as scattering phase functions. It requires complex refractive index of the particle material and the size parameter of the particle, the relation between particle dimension and wavelength, as input. It should be noted, that providing appropriate complex refractive indizes in the THz range even for pure liquid water and water ice is not trivial. This is because very few measurements have been made in this spectral region due to lack of proper light sources and receivers. More details about this issues are discussed in the following section.

Furthermore, an interface to a database by Yang et al.[14] is ready to be used within AMATERASU. The database contains single scattering properties of non-spherical, randomly oriented particles of six different shapes for 45 particle size bins. Aspect ratios of these particles are predefined according to statistics from a vast amount of in-situ data. Spectral optical properties include extinction and absorption efficiency as well as phase functions given from the ultraviolet into the THz range up to 100 μm(=3 THz) on a very fine angular grid of approximately 500 discrete points .

For future, we plan to implement T-matrix code from Mishchenko et al.[15] valid for non-spherical, homogeneous, rotationally symmetric particles. Furthermore, an interface to a database by Rother et al.[16] containing properties of non-spherical particles for a range of size parameters, aspect ratios, and refractive indizes is planned. In addition to the already interfaced and applied version of the Yang et al.[14] database, we will successively implement extensions in the microwave and sub-millimeter region as soon as new data [e.g., [17]] becomes available.

4 Ice dielectric properties

When calculating single scattering properties of particles or extracting them from a material independent database, knowledge of the dielectric properties, e.g., the spectrally dependent complex refractive index (RI), of the forming material is required. With a focus on clouds in the Earth's atmosphere, we currently only plan to consider pure liquid water and water ice in AMATERASU. For the moment, several models are available for water ice that will be described in detail in the following, while implementation of liquid water dielectric properties is pending.

As mentioned before, providing appropriate complex refractive indizes in the THz range even for pure water ice is not a trivial task. Only few measurements have been made within this spectral region due to a lack in light source and receiver technology in the THz region, which is the transistion zone between radio wave and opto-electronic regime. Furthermore, most of the measurements have not been carried out at temperatures where ice clouds detectable with THz instruments usually occur in the Earth's atmosphere. Since RI are usually taken to have only weak temperature dependence at frequencies above approximately 2 THz, this

is not a serious problem for higher THz frequencies. But, below this limit in particular temperature dependence of the imaginary part of the RI becomes significant, i.e., atmospheric RI derived from extrapolating measurements at very low temperatures become less reliable.

Within AMATERASU we implemented five different models for refractive index or permittivity, whose characteristics are summarized in Tab. 1. Out of these models, Warren [18] giving complex values on a discrete grid for the whole range of the electromagnetic spectrum used for remote sensing has become a standard. The values in this model have been compiled from diverse measurements of the imaginary RI in different regions of the electromagnetic spectrum. The real part of the RI has been derived from the spectrally resolved imaginary RI via the Kramer-Kronig-Formula. The other four models are parameterizations, i.e., they give formulas that have been fitted to measurements in certain spectral and temperature regions. Except for Jiang and Wu [19], which has been developed for frequencies up to 3 THz, these parameterized models are defined to be valid in the region up to 1 THz. However, with the exception of Zhang et al. [20] they are more or less based on measurements in the lower frequency region (up to 200 GHz) or at very low temperatures [21]. Warren [18] takes into account few far-IR measurements, but reports on their uncertainty and inappropriate temperature range.

Figures 3 and 4 illustrate the behaviour of all of the five currently implemented RI models in dependence of frequency (Fig. 3) and temperature (Fig. 4) for frequencies up to 1 THz and tropospheric temperatures. For both, temperature and frequency, we find two groups of models–such with linear and such with higher order dependency on the parameter. The Warren [18] model segues from one to the other mode with changing frequency as well as temperature (for the latter even a lower order dependency is found at high temperatures, compare −5 °C curve in Fig. 3). Directly comparing the models with each other (here, Warren [18] has been chosen as reference), significant differences are found for all frequencies and temperatures reaching up to 60 % (see Fig. 5).

In addition to the imaginary part of the RI, Fig. 6 presents the behaviour of the real RI. Deviations between the models here are much lower (below 1 %) and temperature dependence is less significant. Though, it should be noted that Warren [18] derives real RI from applying Kramer-Kronig-Formula, i.e., in a truly physical way, while others assuming a constant real RI [20] or real permittivity [19][22] based on measurement uncertainty of these

Table 1 *Characteristics of ice refractive index models implemented in AMATERASU. UV-MM means ultraviolet to microwave, Perm. is permittiviy, and m. stands for measurements. [1]This column refers to whether dielectric properties are given as complex permittivity $\varepsilon = \varepsilon' - i\varepsilon''$ or complex RI $m = m' - im''$, that are related by $\varepsilon = m^2$. [2]This column denotes, whether the real part of the complex permittivity or RI is given or not. [3]Warren [18] is given on a discrete spectral and temperature grid, not by parameterization formula. [4]Non-constant, discrete values tabulated for a sparse set of frequencies at a single temperature with no comment on temperature dependence. Since differences occur in the forth significant digit only, we use an averaged value for all frequencies and temperatures. [5]Originally, absorptivity is measured and parameterized. Converted into imaginary RI by $\alpha = 4\pi / \lambda \cdot m''$*

name & reference	domain		m or ε[1]	m'/ε' given?[2]	Origin	Parameterization Formula
	freq.[GHz]	T[°C]				
Warren [18]	UV–MM	-60..-1	m	yes	other m.	—[3]
Zhang et al. [20]	250–1000	-35..-10	m	yes[4]	own m.	$m'' = A(m') \cdot f^{-1} + B(T) \cdot f$
Hufford [22]	0–1000	-40..0	ε	yes	other m.	$\varepsilon'' = A(T) \cdot f^{-1} + B(T) \cdot f$
Jiang and Wu [19]	0 3000	-40..0	ε	yes	[21]&[22]	$\varepsilon'' = A(T) \cdot f^{-1} + B(T) \cdot f + C \cdot f^3$
Mishima et al. [21]	240–750	-150..-70	m[5]	no	own m.	$m'' = A(T) \cdot f + B \cdot f^3$

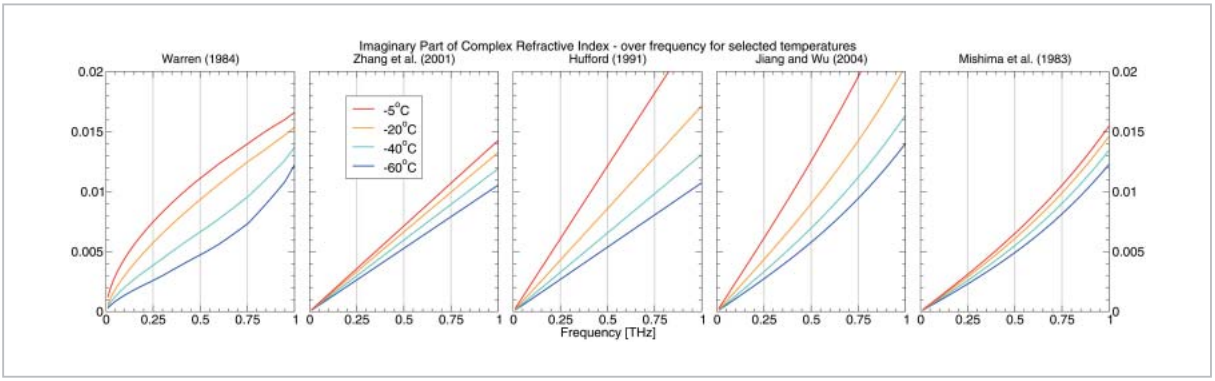

Fig.3 *Imaginary part of complex refractive index in dependence of frequency up to 1 THz for selected ice temperatures plotted separately for the RI models implemented in AMATERASU (see panel header)*

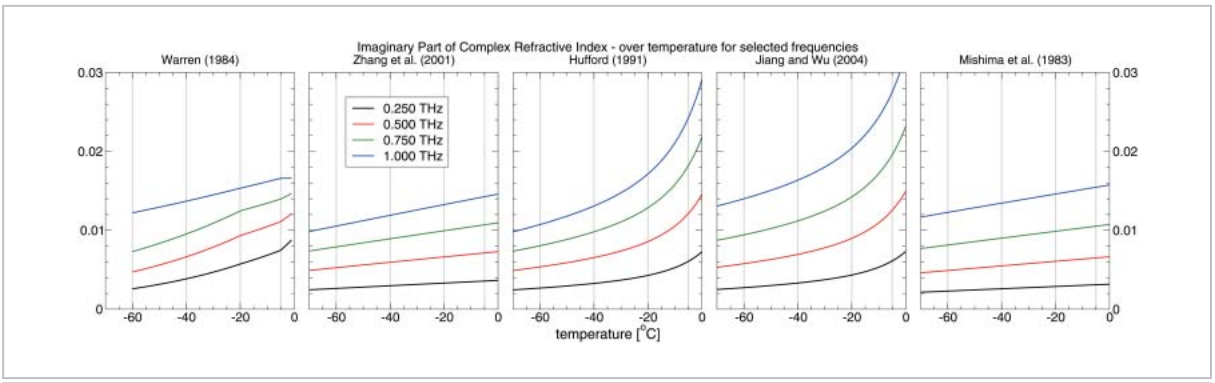

Fig.4 *Imaginary part of complex refractive index in dependence of ice temperature for selected frequencies plotted separately for the RI models implemented in AMATERASU (see panel header)*

values being larger than the change with frequency and temperature. Mishima et al.[21] does not give a statement on real RI at all, but since it is necessary for optical property calculation we applied the value from[20] (because both give imaginary RI while the other two parameterizations provide permittivity) as default in our implementation.

In summary, there exist several models for the lower THz region along with a number of measurements. But, deviations between the models as well as the measurements (for those refer to the original model papers) are quite large. For the higher THz frequency region, the data become very sparse with Warren[18] being the only model above 3 THz. However, due to lack of appropriate accurate measurements, between approximately 3 – 10 THz the Warren[18] model is the best data we can use but not very reliable.

In a further study[23] the sensitivity of cloud ice measurements from sub-mm/THz sensors to uncertainties in the dielectric properties of ice has been analyzed. It has been found, that uncertainties of imaginary RI as large as been found between the examined models are not very critical below 1 THz, but that the rather small real RI deviations cause significant differences in the cloud ice measurements. However, the common and probably most accurate method to derive real RI is the measurement of imaginary RI over a wide spectral range in combination with applying the Kramer-Kronig-Formula as done by Warren[18]. In conclusion, to improve the reliability of clouds ice measurements in this basically very promising spectral region, measurements of dielectric properties in this badly covered frequency range would be of inestimable help. Since THz technology recently has advanced greatly, we can hope for improvements in the near future.

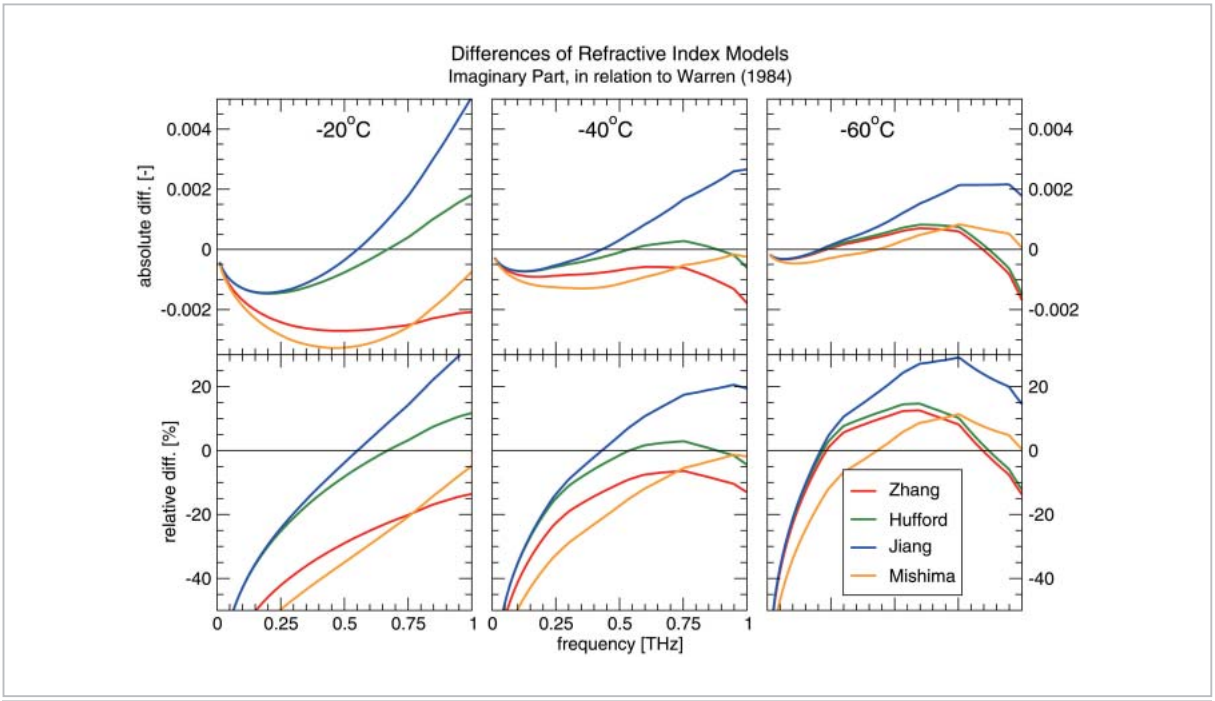

Fig.5 *Differences of RI models implemented in AMATERASU in relation to Warren[18] model. Upper panels show absolute deviations in dependence of frequency for selected temperature. Lower panel present relative deviations.*

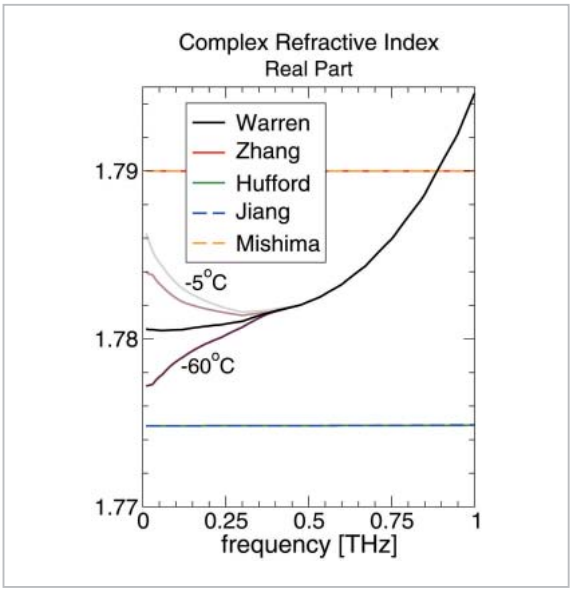

Fig.6 *Real part of the complex refractive index of the implemeted models in dependence of frequency for selected ice temperatures*

5 Summary and conclusions

Modules of the AMATERASU RT model dealing with cases that need consideration of particulate matter, in particular of clouds, have been described. Emphasis has been put on the explanation of approaches, that differ from the ones introduced in Baron et al.[2]. Furthermore, features or data that have recently been implemented to adapt RT algorithms to the requirements of the THz spectral region have been presented in detail and future plans have been pointed out. A special focus has been on discussing the complex refractive index data available for the THz region, which are a crucial parameter to calculate single scattering properties of monodispersions and derive bulk optical properties from these, which are a necessary input to radiative transfer calculations. It has been found, that large discrepancies in the imaginary part exist between the different RI data. But, deviations of top-of-atmosphere intensities and cloud ice measurements derived from these are rather driven by small uncertainties in the real part of complex RI. However, since both are linked and the Kramer-Kronig-Formula allows for the calculation of one of the quantities from measurements in a wider spectral range of the other quantity, accuracy of real RI could be

improved from better, i.e., more frequent and more accurate, measurements of imaginary RI. With new light source and receiver technology at THz frequencies that is under development, e.g., within the THz project at NICT, we possess the tools to perform the necessary laboratory measurements in the near future. This might pave the path to fully exploit the potential of THz sensors for improved measurements of cloud ice, which is still one of the great uncertainties in climate modeling and hydrological cycle[24].

References

1 M. G. Mlynczak, D. Johnson, H. Latvakoski, K. Jucks, M. Watson, D. P. Kratz, G. Bingham, W. A. Traub, S. J. Wellard, C. R. Hyde, and X. Liu, "First light from the Far-Infrared Spectroscopy of the Troposphere (FIRST) instrument", Geophys. Res. Lett., 33, 2006. doi: 10.1029/2005GL025114.

2 P. Baron, J. Mendrok, Y. Kasai, S. Ochiai, T. Seta, K. Sagi, K. Suzuki, H. Sagawa, and J. Urban, "AMATERASU: Model for Atmospheric TeraHertz Radiation Analysis and Simulation", Journal of the National Institute of Information and Communications Technology, in this issue, 2008.

3 J. Urban, P. Baron, N. Lautié, N. Schneider, K. Dassas, P. Ricaud, and J. De La Noë, "Moliere (v5): a versatile forward-and inversion model for the millimeter and sub-millimeter wavelength range", J. Quant. Spectrosc. Radiat. Transfer, 83:529-554, 2004.

4 J. Mendrok, The SARTre Model for Radiative Transfer in Spherical Atmospheres and its Application to the Derivation of Cirrus Cloud Properties, PhD thesis, Freie Universität Berlin, Germany, 2006.

5 A. Kylling, K. Stamnes, and S.-C. Tsay, "A reliable and efficient two-stream algorithm for spherical radiative transfer: Documentation of accuracy in realistic layered media", J. Atmos. Chem., 21:115-150, 1995.

6 A. Dahlback and K. Stamnes, "A new spherical model for computing the radiation field available for photolysis and heating at twilight", Planet. Space Sci., 39 (5):671-683, 1991.

7 K. Stamnes, S-Chee Tsay, W. Wiscombe, and K. Jayaweera, "Numerically stable algorithm for discrete-ordinate-method radiative transfer in multiple scattering and emitting layered media", Applied Optics, 27:2502-2509, 1988.

8 K.-N. Liou, Radiation and Cloud Processes in the Atmosphere, Oxford University Press, New York, 1992.

9 E.P. Shettle, "Models of aerosols, clouds and precipitation for atmospheric propagation studies", In Atmospheric Propagation in the UV, Visible, IR and MM-Wave Region and related Systems Aspects, AGARD Conference Proceedings CP-454, 1990.

10 A. J. Heymsfield and C. M. R. Platt, "A Parameterization of the Particle Size Spectrum of Ice Clouds in Terms of the Ambient Temperature and the Ice Water Content", J. Atmos. Sci., 41(5):846-855, 1984.

11 A. Berk, L. S. Bernstein, and D. C. Robertson, "MODTRAN: A Moderate Resolution Model for LOWTRAN 7", Tech. Rep. GL-TR-89-0122, Air Force Geophys. Lab., Hanscom Air Force Base, MA, 1989.

12 M. Hess, P. Koepke, and I. Schult, "Optical properties of aerosols and clouds: The software package OPAC", Bulletin of the American Meteorological Society, 79: 831-844, 1998.

13 W. J. Wiscombe, "Improved mie scattering algorithms", Appl. Opt., 19:1505-1509, 1980.

14 P. Yang, H. Wei, H.-L. Huang, B. A. Baum, Y. X. Hu, G. W. Kattawar, M. I. Mishchenko, and Q. Fu, "Scattering and absorption property database for nonspherical ice particles in the near-through far-infrared spectral region", Appl. Opt., 44(26):5512-5523, 2005.

15 M. I. Mishchenko, L. D. Travis, and A. A. Lacis, Scattering, Absorption, and Emission of Light by Small Particles, Cambridge University Press, 2002.
16 T. Rother, T. Ernst, J. Wauer, F. Schreier, U. Böttger, and K. Schmidt, "Virtual lab for light scattering and radiative transfer analysis", In 12th International Workshop on Lidar Multiple Scattering Experiments, Volume 5059 of Proceedings of the SPIE, pp.86-94, 2003. doi: 10.1117/12.512340.
17 G. Hong, "Radar backscattering properties of nonspherical ice crystals at 94 GHz", J. Geophys. Res., 112:D22203, 2007. doi: 10.1029/2007JD008839.
18 S. G. Warren, "Optical constants of ice from the ultraviolet to the microwave", Appl. Opt., 23(8):1206-1225, 1984.
19 J. H. Jiang and D. L. Wu, "Ice and water permittivities for millimeter and sub-millimeter remote sensing applications", Atmos. Sci. Let., 5:146-151, 2004. doi: 10.1002/asl.77.
20 C. Zhang, K.-S. Lee, X.-C. Zhang, X. Wei, and Y. R. Shen, "Optical constants of ice Ih crystal at terahertz frequencies", Appl. Phys. Lett., 79(4):491-493, 2001. doi: 10.1063/1.1386401.
21 O. Mishima, D. D. Klug, and E. Whalley, "The farinfrared spectrum of ice Ih in the range 8-25 cm^{-1}, Sound waves and difference bands, with application to Saturn's rings", J. Chem. Phys., 78(11):6399-6404, 1983.
22 G. Hufford, "A model for the complex permittivity of ice at frequencies below 1 THz", Int. J. IR MM Waves, 12(7):677-682, 1991.
23 J. Mendrok, P. Baron, and Y. Kasai, "Terahertz Remote Sensing of Ice Clouds Sensitivity on Ice Dielectric Properties", In Eos Trans. AGU, vol.88(52), Abstract A41B-0444 of Fall Meet. Suppl. AGU, 2007.
24 F. Li, D. Waliser, J. Bacmeister, J. Chern, T. del Genio, J. Jiang, M. Kharitondov, K. Liou, H. Meng, P. Minnis, B. Rossow, G. Stephenand S. Sun-Mack, W. Tao, D. Vane, C. Woods, A. Tompkin, and D. Wu, "Cloud Ice: A Climate Model Challenge With Signs and Expectations of Progress", In Eos Trans. AGU, Vol.88(52), Abstract A42C-04 of Fall Meet. Suppl. AGU, 2007.

***Jana Mendrok**, Ph.D.*
Expert Researcher, Environment Sensing and Network Group, Applied Electromagnetic Research Center
Radiative Transfer Modeling and Cloud Remote Sensing

***Philippe Baron**, Ph.D.*
Expert Researcher, Environment Sensing and Network Group, Applied Electromagnetic Research Center
Development of Forward and Retrieval Models for Atmospheric Remote Sensing

***KASAI Yasuko**, Dr. Sci.*
Senior Researcher, Environment Sensing and Network Group, Applied Electromagnetic Research Center
Terahertz Remote Sensing